



**Global Multivariate Spectral Analysis of Mercury and their Identification of Geochemical  
Terrains: Derived from MASCS Spectrometer onboard NASA MESSENGER Mission**

I. Varatharajan<sup>1</sup>, M. D'Amore<sup>1</sup>, D. L. Domingue<sup>2</sup>, J. Helbert<sup>1</sup>, and A. Maturilli<sup>1</sup>

<sup>1</sup>Institute for Planetary Research, German Aerospace Center DLR, Rutherfordstraße 2, 12489 Berlin, Germany.

<sup>2</sup>Planetary Science Institute, Tucson AZ, 85719, USA.

**Contents of this file**

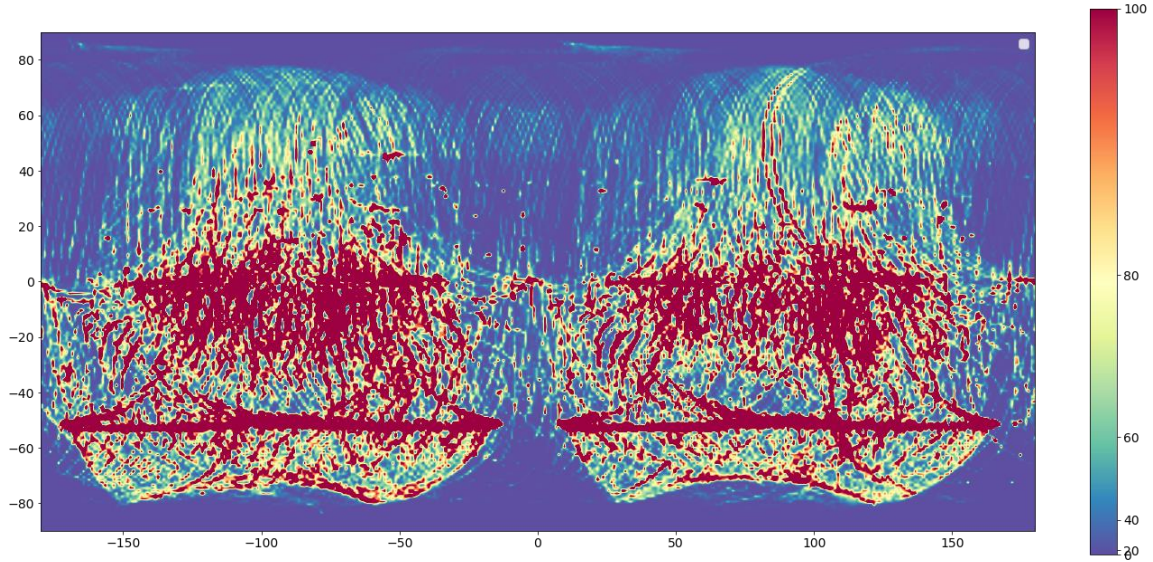
Figures S1 to S4

**Introduction**

The description of each supplementary figure is explained below;

- Figure S1 shows the available number of MASCS spectra per pixel (1°lat x 1°lon) used to create the resulting global MASCS spectral cube. The median of the spectra falling within the spatial resolution of 1°lat x 1°lon is computed to create the global MASCS spectral cube of uniform spatial resolution of 1 pixel per degree (which is equivalent of ~42.5 km/pixel along the equator). Figure highlights the non-uniform spatial distribution of available MASCS spectra.
- Figure S2 shows the variability map at 700 nm. Variability here is defined as standard deviation of the reflectance at 700 nm for the available MASCS spectra per pixel (1°lat x 1°lon) as shown in Fig. S1. Figure shows that only the regions approaching the limited  $\pm 80^\circ$  latitudes show high variability due to the highly variable observational geometry in these zones.
- Figure S3 shows the distribution of visible detector temperature for all observations used in this study. These distribution does not produce any of the features seen in global maps including the variability map in Fig. S2. This further confirms that there are no instrumental artifacts that affects the spectral analysis in the study.

- Figure S4 shows the random K-means clustering map for each k values i.e., number of clusters where  $k=2,3,4,5,6,7,8,9,10,20$  and its corresponding histogram showing the number of pixels per cluster for each k. S4 shows that irrespective of the k value, most of Mercury surface fall into two contiguous regions.



54

55 **Figure S1.** The available number of MASCS spectra per pixel ( $1^\circ\text{lat} \times 1^\circ\text{lon}$ ) used to create the  
 56 resulting global MASCS spectral cube represented on the colormap which uses power law  
 57 scale ( $y=x^y$ , where  $y=3$ ). Figure highlights the non-uniform spatial distribution of available  
 58 MASCS spectra per pixel per degree (which is equivalent of  $\sim 42.5$  km/pixel along the equator).  
 59 In order to create the global MASCS datacube of uniform spatial resolution of 1 pixel per  
 60 degree used in the study, the median of the spectra falling within this spatial resolution of  
 61  $1^\circ\text{lat} \times 1^\circ\text{lon}$  is computed.

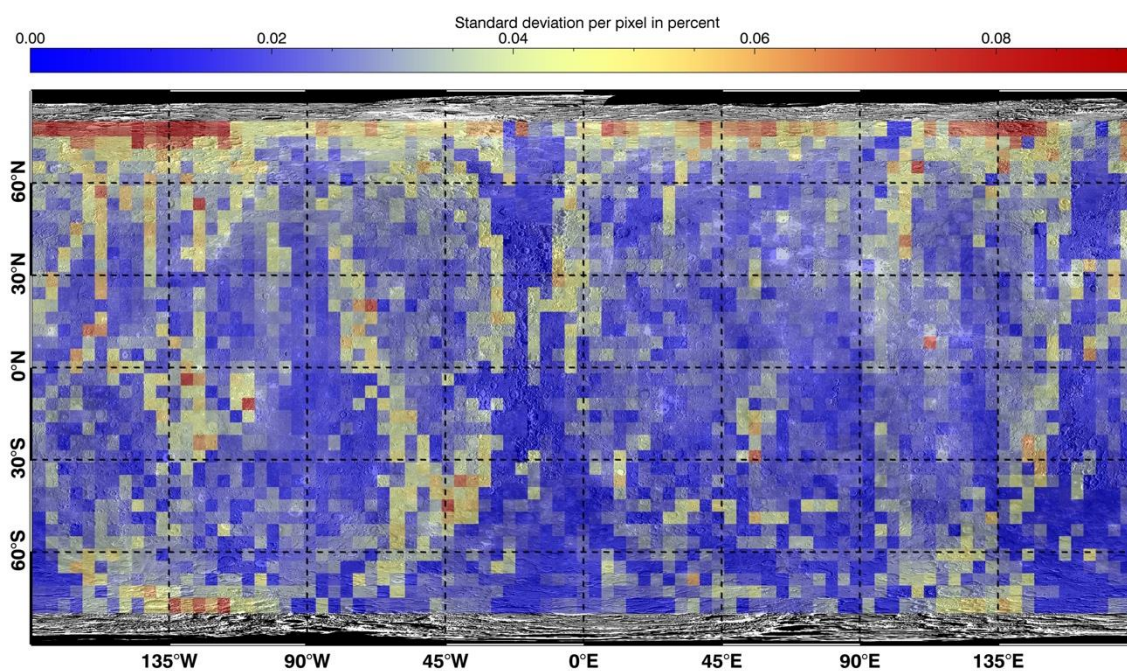


**Figure S2.** Shows the variability map at 700 nm. Variability here is defined as standard deviation of the reflectance at 700 nm in percentage for the available MASCS spectra per pixel (1°lat x 1°lon) as shown in Fig. S1. Figure shows that only the regions approaching the limited  $\pm 80^\circ$  latitudes show high variability due to the highly variable observational geometry in these zones.



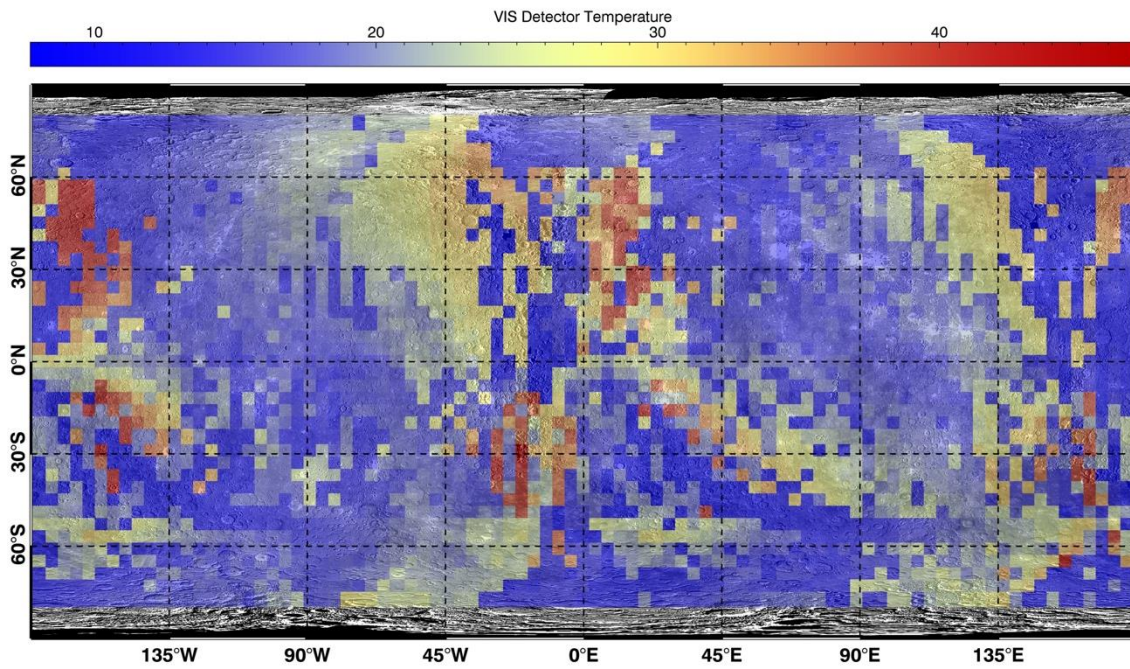


**Figure S3.** Shows the distribution of visible detector temperature for all observations used in this study. These distribution does not produce any of the features seen in global maps including the variability map in Fig. S2. This further confirms that there are no instrumental artifacts that affects the spectral analysis in the study. The visible detector temperature data is available in the downloaded MASCS spectra from PDS.

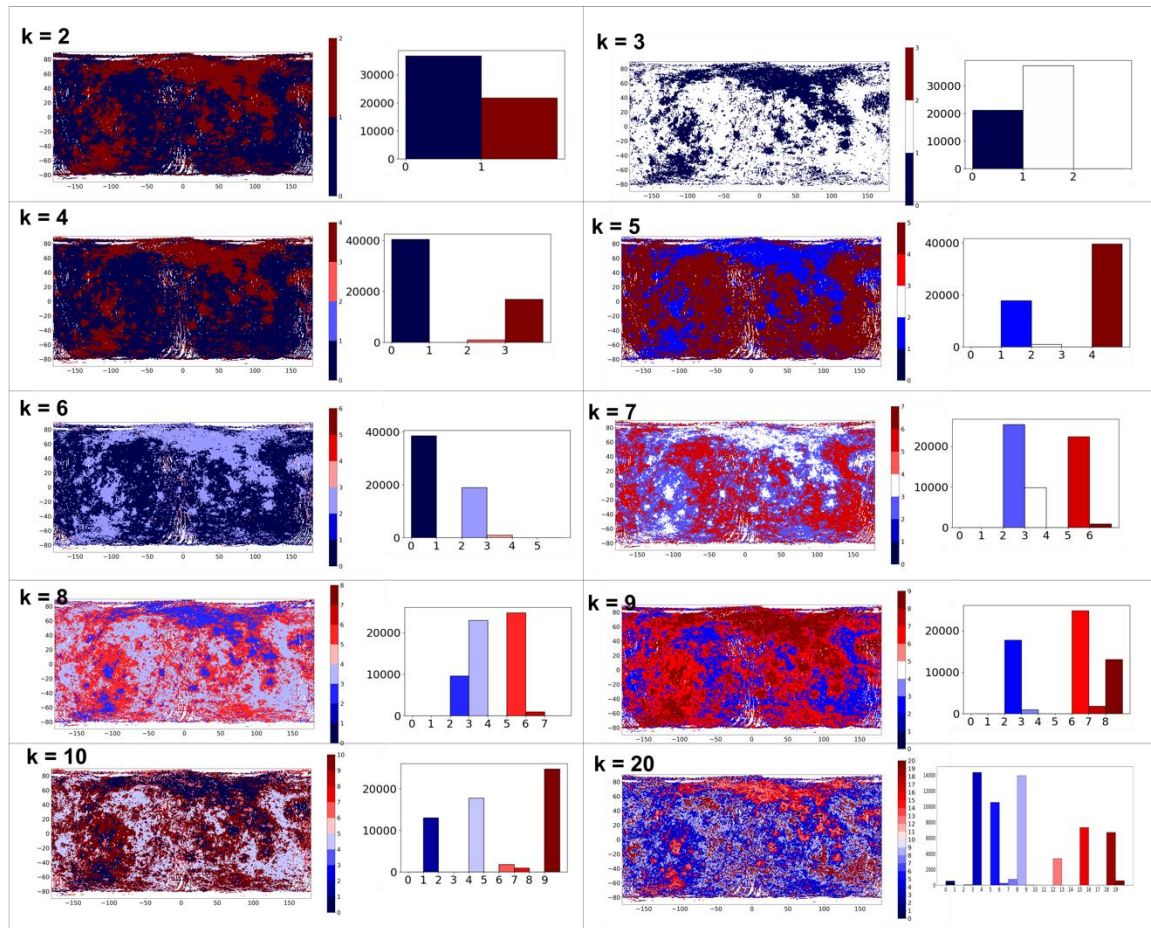


**Figure S4.** Shows the random K-means clustering map for each  $k$  values i.e., number of clusters where  $k=2,3,4,5,6,7,8,9,10,20$  and its corresponding histogram showing the number of pixels per cluster for each  $k$ . It shows that irrespective of the  $k$  value, most of Mercury surface fall into two contiguous regions.